

Interactive needle insertions in 3D nonlinear material

Han-Wen Nienhuys

A. Frank van der Stappen

institute of information and computing sciences, utrecht university

technical report UU-CS-2003-019

www.cs.uu.nl

Interactive needle insertions in 3D nonlinear material

Han-Wen Nienhuys and A. Frank van der Stappen

Abstract

In this paper, we show an interactive simulation of needle insertions in both 2D and 3D and soft tissue. The approach is based on the Finite Element Method (FEM) and uses quasi-static stick-slip friction for needle/tissue interactions. The FEM equations are solved using an iterative method, and the mesh is refined adaptively near the needle trajectory. The boundary formed by the needle surface is not represented explicitly in the mesh, but its geometry is accounted for in the friction forces. Since the surface is not represented explicitly, the quality of the initial mesh can be maintained by using a simple refinement scheme. This approach can also be applied to both the 3D situation and nonlinear material models. We present results of computational experiments of the 2D simulation, and show samples of the 3D implementation.

1 Introduction

Inserting needles into soft tissue is one of the most often performed medical procedures. In some procedures, needles have to be inserted deeply into soft tissue to reach a target. For example, certain types of biopsies are performed with needles with a specialized tip, designed to extract a tissue specimen. Another application is *brachytherapy*, treating cancer by inserting radioactive seeds directly in the tumor. The primary application of brachytherapy is prostate cancer. In this application the seeds are delivered with a needle. When a needle is inserted into soft material, such as tissue, the material and the needle interact through friction forces, resulting in deformation of the material. In a clinical setting, this deformation makes it harder to reach the desired target and avoid vital organs. Simulations of needle insertions that take into account tissue deformation may help train and plan for such difficult cases.

Simulations of needle insertion for training purposes have been implemented earlier using ad-hoc models, e.g. [2], which rely solely on force measurements performed at the inserting end. The work by DiMaio and Salcudean [3, 4] presents a breakthrough. They present a planar virtual environment for needle insertion. The simulation uses a static linear finite element model, and achieves haptic rates on a Pentium3/450Mhz by precomputing the response of the system by means of *condensation*. Friction forces along the needle shaft are derived from measurements of the complete 2D deformation field. Alterovitz et al. [1] also simulate needle insertion using the FEM, and specifically target brachytherapy for prostate cancer treatment. They use a linear elasticity model on a uniform 2D grid, but use an explicit GN22 integration scheme to dynamically solve these equations. The model runs at visual update rates (25 Hz) for a uniform 1250 triangle mesh on a Pentium3/750Mhz.

Unfortunately, generalizing these approaches to 3D increases the problem size such that uniform meshes are no longer feasible. In a two-dimensional setting, the boundary is one-dimensional, and can be represented accurately by a small set of edges. In physically valid 3D discretizations, forces, such as friction, are applied to surfaces. Therefore, the needle must be represented in the mesh as a surface in 3D. To represent this surface adequately, the mesh must include elements with a size comparable to the needle diameter. A simple computation shows that a uniform mesh—necessary for condensation—with elements of size 1mm for a 10 cm \times 10 cm \times 10 cm object leads to a stiffness matrix with roughly $3 \cdot 10^6$ degrees of freedom. Condensation of internal nodes requires storing the inverse of the stiffness matrix, which is dense and occupies approximately 67 terabytes of memory.

We propose a solution to simulating needle insertions based on *iterative algorithms*. Such algorithms do not require precomputed structures, implying that the mesh may be changed at run-

time. In particular, the mesh can be *refined adaptively* in the region of interest, thus ensuring that the discretization is accurate while computational requirements remain low. Moreover, iterative algorithms can also handle *nonlinear material models*, which are necessary to accurately predict the results of large deformations [8]. Incorporating arbitrary boundaries, such as the needle surface, while maintaining high mesh quality can be difficult, especially in 3D [9]. However, in our case there is no special reason to represent that boundary exactly. By accounting for the geometry of the needle surface in the magnitude of the friction forces, we can compute the effect of friction. We refer to this as a *nonconforming* method. Since no complex meshing techniques are necessary, we can use a simple subdivision scheme. It exactly maintains element shapes of the starting mesh, ensuring that the refined mesh has a *high quality*, and leads to an accurate discretization.

In the rest of the paper, show how an iterative algorithm, adaptive meshing and nonconforming method are combined to produce a needle insertion simulation that achieves high precision at low computational costs, and also generalizes to 3D, nonlinear material. These techniques have been used to produce a 2D simulation that is functionally equivalent to the one shown by DiMaio and Salcudean. With our method, it is possible to exchange computation time and accuracy. Computational experiments indicate that in 2D this method runs at haptic update rates for displacement accuracies of approximately 1 mm. Our method generalizes to 3D objects with nonlinear elasticity, and we show a sample from the prototype 3D implementation.

2 Physical model

The mechanical behavior of 2D tissue itself is governed by equations for two-dimensional elasticity, so-called *plane stress* [10]. For problems where loads and deformations occur in a plane, one coordinate can be removed from the 3D elasticity formulation. In the case of a flat slab of material, stresses in the third coordinate vanish. The elastic responses in the remaining 2 coordinates are similar to the 3D responses, albeit with a different reaction to strains that change volume. For linear material, the 2D second Piola-Kirchoff stress tensor $\tilde{\mathbf{S}}$ equals $\mu(\tilde{\mathbf{C}} - \tilde{\mathbf{I}}) + \frac{2\mu\lambda}{\lambda+2\mu} \text{trace}(\tilde{\mathbf{C}} - \tilde{\mathbf{I}})\tilde{\mathbf{I}}$, where λ and μ are the Lamé parameters, $\tilde{\mathbf{C}}$ is the right Cauchy-green strain tensor, and $\tilde{\mathbf{I}}$ the identity. For nonlinear materials, the same procedure may be used to derive 2D constitutive equations. When the material is presumed not to conserve volume at all (i.e., $\lambda = 0$), then compressible neo-Hookean material [10] has the following stress-strain relation for the plane stress case,

$$\tilde{\mathbf{S}} = \mu(\tilde{\mathbf{I}} - \tilde{\mathbf{C}}^{-1}). \quad (1)$$

For small deformations, the neo-Hookean model reduces to the linear material model.

The interaction between the needle and the tissue is a form of *stick-slip* friction. When the needle moves slowly, material sticks to the needle. At higher speeds the material slips across the needle. Hence, the needle forms a part of the boundary where either displacements (stick friction) or tractions (slip friction) are prescribed. The magnitude of the friction depends on the difference between the velocity of the needle and the material. This relation is discontinuous, which leads to numerical problems in a dynamic formulation. Therefore, we use a quasi-static formulation. Nodes that lie on the needle, *needle nodes*, can have two states: either a node is fixed (sticking), which means that its location is attached to the user controlled needle, or its movement is constrained to be parallel to the needle shaft (slipping). A configuration of slipping and sticking nodes leads to a single static deformation problem. When the solution of this problem is found, the elastic reaction forces can be used to rearrange the boundary conditions. Needle nodes whose elastic force exceeds the friction threshold are marked as slipping, and the others are marked as sticking.

We will discretize the elasticity problem using the Finite Element Method [10] on a triangle mesh. As we explained above, the needle surface is part of the boundary of the domain. In a *conforming* finite element method, the boundaries of the domain should be represented exactly. This implies that the needle should be represented in the mesh by a connected set of connected edges in 2D, or by a set of faces in 3D. This can be achieved by relocating existing mesh nodes in the reference mesh, by moving nodes in the deformed mesh, thus introducing extra stresses, or

by subdividing the elements while inserting new nodes. Neither relocating or deforming nodes in the mesh, nor unjudicious use of subdivision decreases the element size locally, so in general, these methods will not improve the accuracy of the solution. This motivates us to experiment with a nonconforming scheme, where nodes are not moved within the mesh. Instead of adapting the geometry to include the needle shape in the mesh, the geometry is left unchanged, and the friction forces are adjusted based on geometry. In 2D, nodes close to the needle shaft are considered to be needle nodes. The friction forces on needle nodes are computed based on the distance component parallel to the needle shaft. In 3D, tetrahedra close to the central axis of the needle are considered to be part of the needle. The boundary of this set of tetrahedra is projected onto the needle, and the area of the projection is used to compute forces. Both procedures are illustrated in Figure 1.

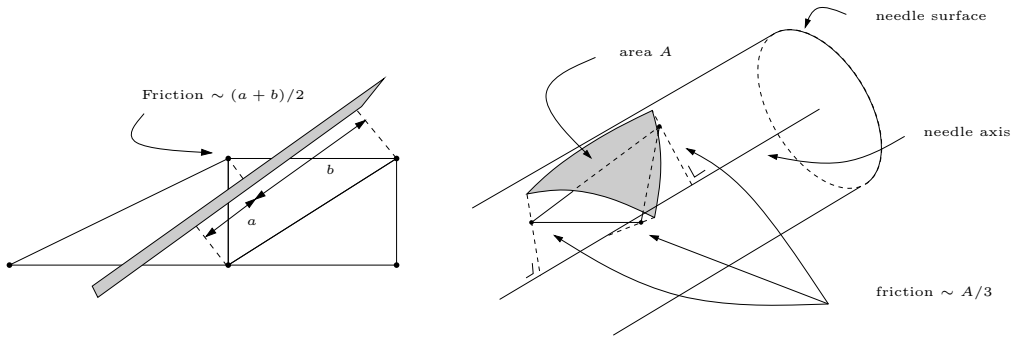


Figure 1: Accounting for the needle/mesh geometry interaction through the forces. In 2D, nodal friction forces are proportional to the distance parallel to the needle. In 3D, triangles are projected on the surface of the needle (indicated in grey). Friction forces are proportional to the projected area.

3 Implementation

We will consider a square object that can be meshed with regularly arranged right-angled triangles, as shown in Figure 3. This is not an essential restriction, but it does ease the discussion and the implementation. To increase accuracy, the resolution of the mesh is locally increased near the needle. This refinement is done using *edge bisection*: a triangle is refined by splitting the longest edge. By recursively splitting neighboring triangles in the same manner, mesh compatibility is maintained. This scheme is easy to implement, and maintains element quality. It is illustrated in Figure 2. This scheme is easy to extend to tetrahedral meshes [5], which is also illustrated in Figure 2.

We use the Conjugate Gradient (CG) method [7] for solving elasticity equations. This method is more efficient than dynamic relaxation using lumped masses [6], and has no stability problems. The CG method can be applied to both linear and nonlinear elasticity, and can cope with changing boundary conditions. It can be implemented using a matrix-free setting, so there is no need to store precomputed structures. The method decreases potential energy until the following stopping criterion is achieved

$$\|f^{\text{extern}} + f^{\text{elastic}}\|_2 < \varepsilon \sqrt{\|f^{\text{extern}}\|_2^2 + \|f^{\text{reaction}}\|_2^2}.$$

The tolerance ε controls the *relaxation error*: the lower ε , the more accurate the numerical solution. The quantities f^{elastic} , f^{extern} and f^{reaction} are the \mathbb{R}^{2n} vectors (\mathbb{R}^{3n} in 3D) containing elastic forces, externally applied forces, and reaction forces (e.g., forces required to keep sticking nodes in their fixed positions) for every node.

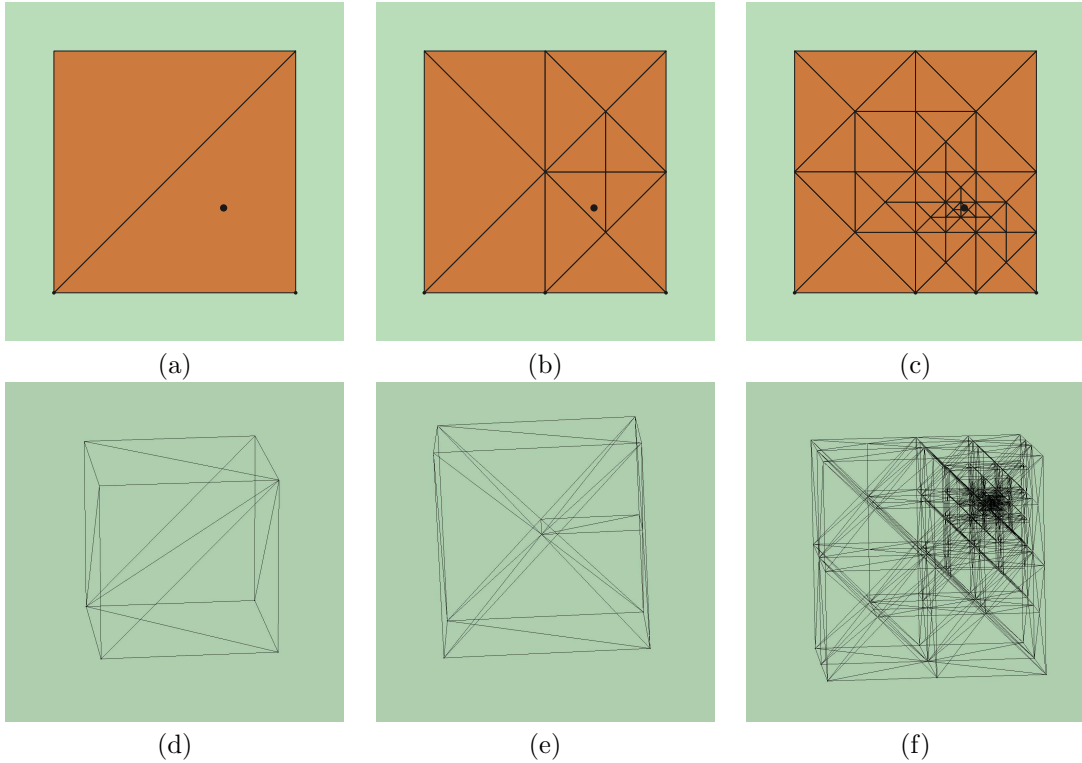


Figure 2: Recursive edge bisection, with refinement around a single point. Picture (a) shows the starting mesh. Picture (b) and (c) shows the effect of 5 and 10 refinements. Pictures (d), (e) and (f) show 0, 3 and 20 refinements in 3D.

4 Computational experiments

By conducting computational experiments, we can assess whether this approach is practically feasible. As far as the physical model is concerned, both our scheme and the one of DiMaio and Salcudean are equivalent, since they use the same elasticity model and friction parameters. Hence, the question is: how accurate is the system for a given amount of computation?

By experimenting on a standardized object, (a slab with dimensions $0.10 \times 0.10 \times 0.01$ m, and material properties $E = 34$ kPa, $\nu = 0.34$), we have found [6] that displacement errors of approximately 1 mm can be attained by refining elements to size $2^{-6} \cdot 0.1$ m in the vicinity of the needle, using a starting mesh with edge lengths around $2^{-3} \cdot 0.1$ m. The conformance error, caused by representing the needle surface precisely, is smaller than the discretization error. The relaxation error, introduced by using the iterative CG algorithm, is small: very moderate values (0.1) for ε are needed to make displacement errors smaller than discretization errors. For these settings, the deformation engine achieves an average update rate in excess of 700 Hz on a Pentium3/1Ghz.

Our solution method does not exploit the linearity of the problem. Hence we can also use nonlinear material models. In Figure 3 a scenario is shown that involves large deformations. The needle is inserted sideways into a slab of material fixed at the bottom. The needle describes a trajectory that is curved relative to the object in its rest configuration. The material is set to have Poisson ratio $\nu = 0$, so Equation (1) applies, and the simulation can be done both with neo-Hookean and linear elasticity. The difference between the final location of the needle tip in both experiments is approximately 8 mm, which is significantly larger than the all other errors analyzed. Update rates for the nonlinear experiment are a factor 2 lower.

The 2D system was designed with the intent of generalizing to three dimensions. This generalization has also been implemented in a prototype, and samples are shown in Figure 4. In 3D,

smaller elements are necessary to approximate the needle surface correctly. In the case of Figure 4, almost 30,000 elements were necessary, an increase of a factor 47 over the example in Figure 3. Since 3D matrix operations are also 2 to 3 times as expensive, the total computational cost of a 3D simulation is roughly a factor 120 larger.

5 Discussion

In this paper we have presented a novel method for computing deformations during simulated needle insertions into 2D and 3D elastic material. The method builds on previous work by its use of a quasi-static model of stick/slip friction with 2D plane-stress elasticity. It is different in that it uses an iterative (and optionally nonlinear) relaxation algorithm, and adaptive mesh resolution, making a generalization to 3D possible. The mesh used has a high degree of regularity, and is refined near the inserted needle to improve the local accuracy. Nodes are not moved within the mesh, so the refinement technique, edge bisection, does not cause element shape deterioration.

To assess the cost/accuracy ratio of this method, the 2D method was implemented in a prototype and subjected to a number of computational experiments. The performance of the method is related to coarseness of the mesh, and material model used. Both factors are related to the accuracy of the end-result, so it is possible to improve response times by sacrificing accuracy. We conclude that accuracies around 1 mm for insertion in linearly elastic objects of size 10×10 cm can be achieved at haptic update rates on a 1 Ghz PC. At these rates, the discretization error (caused by coarseness of the mesh), conformance error (caused by our nonconforming scheme), relaxation error (caused by using an iterative algorithm), and rounding errors taken together are below 1 mm. Given the result of our experiment with neo-Hookean elasticity (which introduced a difference of 8 mm), we see that a good tissue model is crucial to making accurate predictions of tissue deformations. Therefore, research into improvements in computational techniques should be accompanied by a more in-depth analysis of the mechanical properties of the organs being modeled. A complete analysis should also include sensitivity to needle flexion (we assume the needle to be rigid) and variation in material parameters.

We have conducted tests with square slabs and cubes as deformable objects. This simplifies implementation, but it is not an essential restriction: the only requirement successful for recursive edge bisection, is that vertices of the original grid are ordered [5].

Our approach generalizes to 3D. This 3D generalization has also been implemented, thus showing its feasibility. However, the computational costs of a 3D simulation are too high for haptic applications. Iteration counts of the CG algorithm are very low in both the 2D and 3D simulation. This can be explained by the high spatial coherence between subsequent solutions and limited mesh resolution outside the region of interest. This suggests speed-ups should not be sought in techniques that decrease CG iteration counts (such as preconditioning and multigrid techniques), but in techniques that improve raw computation power: dedicated hardware and parallel processing.

References

- [1] Ron Alterovitz, Jean Pouliot, Richard Taschereau, I-Chow Joe Hsu, and Ken Goldberg. Simulating needle insertion and radioactive seed implantation for prostate brachytherapy. In J. D. Westwood et al., editor, *Medicine Meets Virtual Reality 11 (MMVR11)*, pages 19–25. IOS Press, January 2003.
- [2] P. N. Brett, T. J. Parker, A. J. Harrison, T. A. Thomas, and A. Carr. Simulation of resistance forces acting on surgical needles. *Journal of Engineering in Medicine*, 211(13):335–347, September 1997.
- [3] S. P. DiMaio and S. E. Salcudean. Needle insertion modelling and simulation. In *IEEE International Conference Robotics and Automation (ICRA)*, 2002.

- [4] S. P. DiMaio and S. E. Salcudean. Simulation of percutaneous procedures. In T. Dohi and R. Kikinis, editors, *Medical Image Computing and Computer Assisted Intervention (MICCAI)*, number 2489 in LNCS, pages 253–260. Springer-Verlag, 2002.
- [5] Joseph M. Maubach. Local bisection refinement for n -simplicial grids generated by reflection. *SIAM Journal for Scientific Computing*, 16(1):210–227, January 1995.
- [6] Han-Wen Nienhuys. *Cutting in deformable objects*. PhD thesis, Utrecht University, 2003.
- [7] Jorge Nocedal. Theory of algorithms for unconstrained optimization. *Acta Numerica*, 1:199–242, 1992.
- [8] G. Picinbono, H. Delingette, and N. Ayache. Non-Linear Anisotropic Elasticity for Real-Time Surgery Simulation. *Graphical Models*, 2002. In press.
- [9] Jonathan Richard Shewchuk. A condition guaranteeing the existence of higher-dimensional constrained Delaunay triangulations. In *Annual ACM Symposium on Computational Geometry*, pages 76–85. Association for Computing Machinery, 1998.
- [10] O. C. Zienkiewicz and R. L. Taylor. *The Finite Element Method*, volume 1 and 2. Butterworth-Heinemann, 2000.

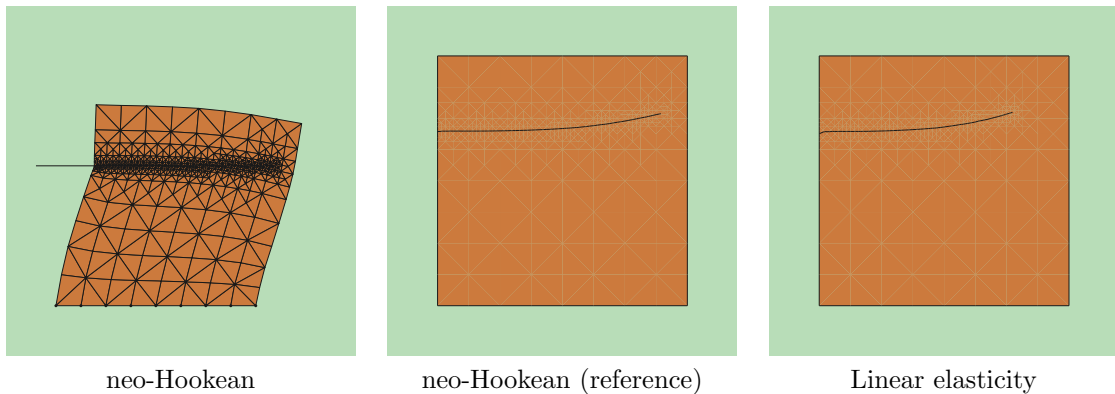
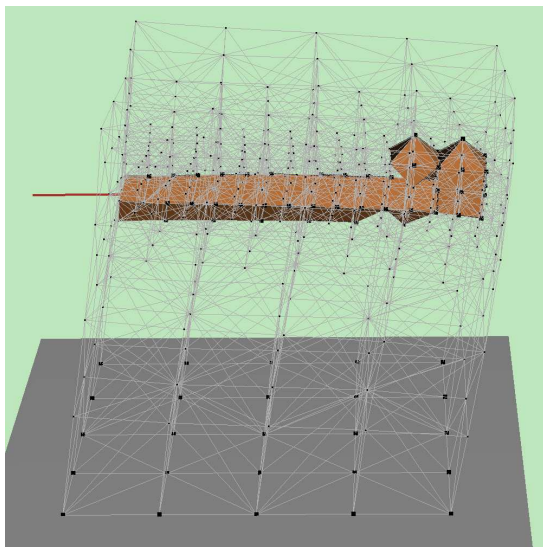
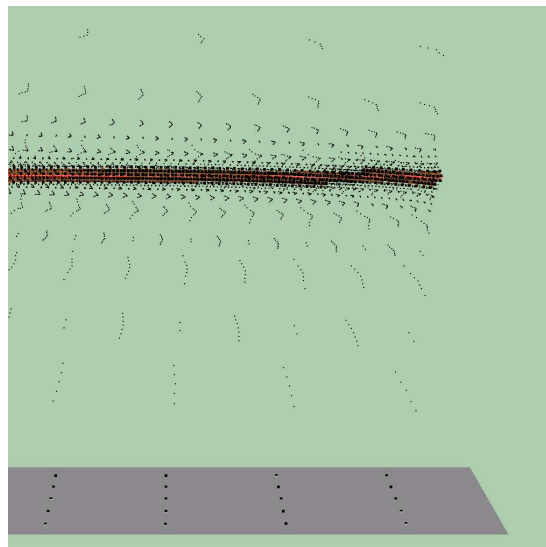


Figure 3: Neo-Hookean (left and center) linearly elastic material (right) compared. A needle insertion sideways into slab of elastic material ($10\text{ cm} \times 10\text{ cm}$) Poisson ratio $\nu = 0$) fixed on the bottom was simulated for two material models. The left picture shows the deformed configuration for neo-Hookean material, the center and right picture the reference configurations for neo-Hookean and linear material. The distance between the tip location in both reference locations in both experiments is approximately 8 mm. The simulation for the nonlinear case took approximately 38 seconds on a P3/1Ghz and ended with a mesh of 625 elements.



linear elasticity
5 seconds (P3/1 Ghz), 2420 elements



neo-Hookean material
1364 seconds (P3/1Ghz), 29562 elements

Figure 4: Insertions of a needle (radius 1 mm) from the left into a elastic cube ($10\text{ cm} \times 10\text{ cm} \times 10\text{ cm}$) fixed on the bottom. The needle surface is drawn solid; the surface is jagged, but the result remains valid due to how forces are chosen. Left: linear material, 12 fold refinement around the needle. On the right a detail from a similar insertion into neo-Hookean material, with 20 fold refinement around the needle (Mesh edges are not shown). Timings were done on a P3/1Ghz. The needle exits the object in the right picture, but doesn't in the left one, again showing that material model and mesh resolution can affect the outcome of a simulation.